Journal of New Technology and Materials
JNTM
Vol. 07, N°01 (2017)90-96

OEB Univ. Publish. Co.

Optimization of the Raw Material Input Molar Ratio on the Carbothermal Production of Solar-Grade Silicon

Rabie Benioub[a,b,*], Mohamed Adnane[b], Abderahmane Boucetta[a], Amina Chahtou[a], Hidekazu Kobatake[a], Yasubumi Furuya[a] and Kenji Itaka[a]

[a]*North Japan Research Institute for Sustainable Energy, Hirosaki University, 2-1-3, Matsubara, Aomori, 030-0813, Japan*
[b]*Université des Sciences et de la Technologie d'Oran Mohamed Boudiaf, USTO-MB, BP 1505, El M'naouer, 31000 Oran* Algérie
*Corresponding authors, E-mail: dr_b_r@yahoo.fr
Received date: March 09, 2017; revised date: June 15, 2017; accepted date: June 17, 2017

Abstract

With the fast growth of solar cells market, it is strongly required to improve the fabrication process of solar-grade silicon, which is the base material for more than 93% of solar cells technology. Conventionally, solar-grade silicon is produced via the direct reduction of silica stone to metal-grade silicon by arc furnace followed by the Siemens method with chemical treatment and hydrogen. However, in this technique a low yield of solar-grade silicon is obtained with high energy cost due to its multiple complex processes. Meanwhile, it has been turned out that, the direct reduction process from silica sand to solar-grade silicon via induction furnace simplify the fabrication process with low energy and cost consumption with higher yield. In this study, the optimum partial pressure and temperature conditions of this process were based on the stability phase diagram for reduction reaction process. Using the simulation results, we succeeded to increase the reduction yield by ten times.

Keywords: Carbothermic silica reduction;Solar-grade silicon; Raw material ratio; Reduction yield.

1. Introduction

As the first material for solar cells fabrication, solar-grade silicon (SoG-Si, around 6N) has been produced via the carbothermic reduction process using an electric furnance [1]. Silica from gravel and stones and carbon from charcoal, wood chips, coal, and coke, were used as raw materials in the silicon production process which requires high temperatures and much energy [2]. Various route for silicon production have been investigated, including the Siemens as shown in Figure 1 (a), starting by a direct reduction in an arc furnace of silica stone by carbon to get metallurgical-grade silicon with a huge amount of CO_2 gas released, and followed by a reduction of $SiHCL_3$ gas using hydrogen gas[3-6]. In addition, other methods such as Union Carbide, Fluidized bed processes and electrolytic were used too[7,8]. However, some of these processes includes multiples processes which make the application of these methods complicated. Therefore, the high purity direct carbothermic reduction process which represents a new method of production of low-cost SoG-Si expresses less time and energy consumption as shown in Fig. 1(b). This method includes a two-step conversion processes, statring by extraction of pure silica (SiO_2) from silica sand with raw purity of 97% and 99.9% (3N) after purification[9], and followed by direct carbothermal reduction of this pure silica in an induction furance for production of silicon[10]. However, this method expressed a low reduction yield[11,12]. Therefore, the understanding of the phase diagram of the direct carbothermic silica reduction process, and the estimation of by-product such as SiO and CO gases partial pressure is inevitable for the improvement of the direct reduction. Moreover, previous report show a solid relationship between the raw material input such as silica and carbon and the final product such as Si and SiC [13-15]. However, the dependency on raw material input of the total mass balance of the reduction process which represent a total understanding of the different material conversion and total mass preservation related the solid-gas form conversion were not discussed before.

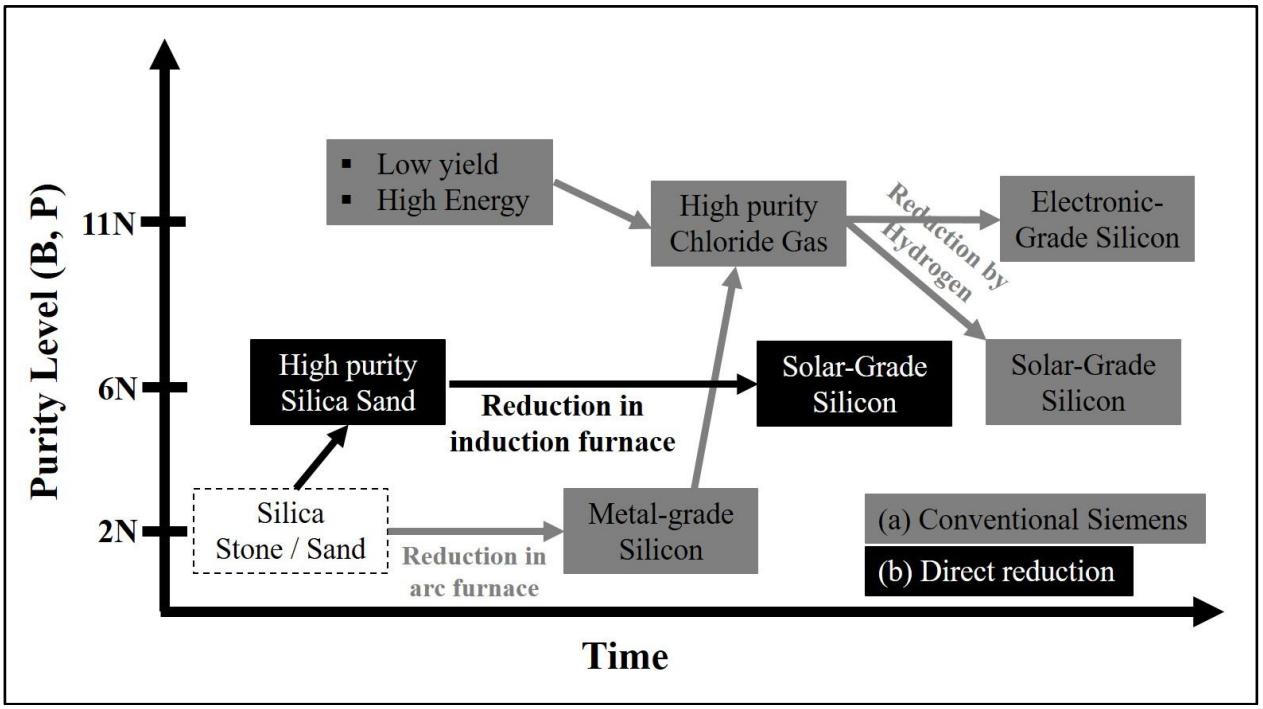

Fig. 1 Schematic comparison between conventional Siemens method through direct reduction process from silica stone to metal-grade silicon (a) and the main target of this research work which is the direct reduction process from silica sand (b).

In this research work, the phase diagrams of the direct carbothermal reduction possible reaction were simulated and discussed as a function of partial pressure of SiO to CO gasses using thermodynamic calculation of Gibbs free energy. The optimum temperature and partial pressure of SiO/CO were deduced from the simulation results and used in experimental work to confirm the effect of mole ratio variation between SiO_2 and Carbon raw material on the solid-gas conversion efficiency known as the reduction yield.

2. Simulation and Experimental Procedure

2.1. Si-O-C Phase Stability Diagram

The simplified overall reaction in the reduction process are shown below in equations (1-5) below, show the overall reaction in silicon production, which requires knowledge about the reaction at high-temperature zones of the furnace[16].

SiO_2 (s) + C (s) = SiO (g) + CO (g)..... .....(1)

$\Delta G^\circ = 668.07 - 0.3288T(\text{kJ})(1273\text{K} \le T \le 1993\text{K})$

$2SiO_2$ (s) + SiC (s) = 3SiO (g) + CO (g).....(2)

$\Delta G^\circ = 1415 - 0.6586T(\text{kJ})(1273\text{K} \le T \le 1993\text{K})$

SiO (g) + 2C (s) = SiC (s) + CO (g).....(3)

$\Delta G^\circ = -78.89 + 0.0010T(\text{kJ})(1273\text{K} \le T \le 2273\text{K})$

SiO (g) + SiC (s) = 2Si (s) + CO (g)..... .....(4)

$\Delta G^\circ = 165.56 - 0.0751T(\text{kJ})(1673\text{K} \le T \le 2273\text{K})$

SiO_2 (l) + Si (l) = 2SiO (g)..... ....(5)

$\Delta G^\circ = 616.37 - 0.2875T(\text{kJ})(1673\text{K} \le T \le 2273\text{K})$

where, ΔG° represents the standard Gibbs energy of each reaction. (s), (l) and (g) referred to solid, liquid and gas phases.

In this process to produce silicon, a reaction temperature higher than 1500℃ (1773K) to produce enough SiO gas through reaction (1) and (2). Phase stability diagrams for the reactions in Eqs. (1-5) were calculated as illustrated in Figure 2 (a-d) with the standard Gibbs energy of the reactions taken from MALT2[17].Our main target was focused on the partial pressure ratio of SiO gas to CO gas because of its possible experimental occurrece as shown in Figs. 2 (a-d) with black dashed horizontal lines. In the carbothermic process of silicon, silica will start to react with carbon at a temperature over 1054°C(1327K) as increasing temperature with generation SiO gas Eq. (1) which is shown as the first gray color in Fig. 2 (a). While silicon carbide starts to react with carbon in Eq. (2) at 1070℃ (1343K) to generate SiO corresponding to the first gray color in Fig. 2 (b). As for the reactions in Eqs. (3), (4) and (5), silicon carbide is generated via Eq. (3) with the interaction between SiO gas and carbon, and thermodynamically the reaction proceeds even at low temperature but experimentally it is difficult because its required rich SiO gas pressure generated from the previous reactions[18]. Si is produced by the reaction of silicon carbide with SiO gas at the temperature of 1500℃ (1773K) via Eq. (4)[19]. While si production from SiO2 releasing of SiO gas Eq. (5) could be occurred at very low temperature below 1400°C(1673K) due to requirment of the presence of liquid silica and silicon forms at lower temperature. Colorless area below at lower temperature corresponds to no reaction in Figs. 2 (a-d) due to the negligible partial pressure of SiO(g) and CO(g) due to the presence of solid silica and carbon[20, 21].

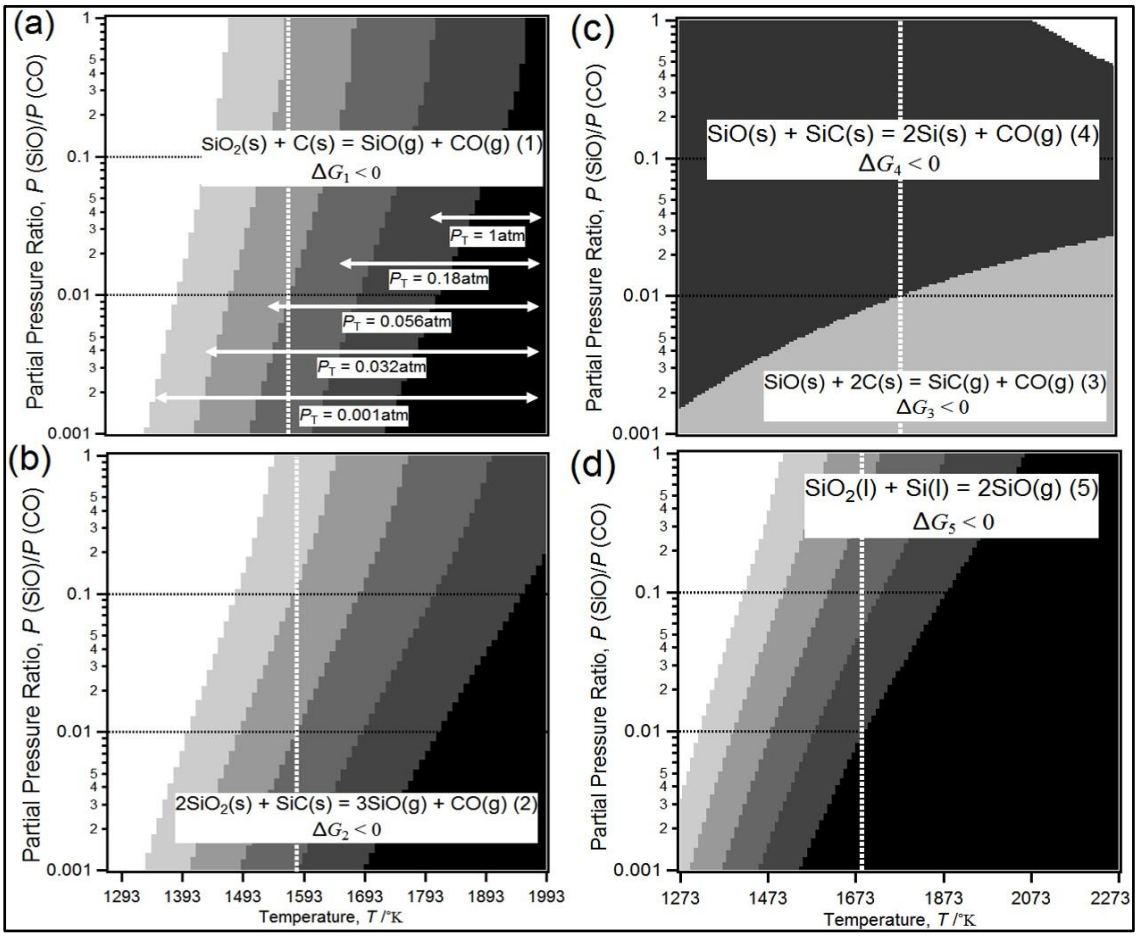

Fig. 2 Si-O-C Phase stability diagram for the ratio of SiO/CO gas phases: (a), (b), (c), and (d) for reactions in Eqs. (1), (2), (3), (4) and (5). This diagram shows the variation of the partial pressure ratio SiO/CO and temperature impact on the reduction of silica to silicon based on calculated data from MALT2.

Therefore, our system, the partial pressure ratio of SiO and CO range is between 0.01 to 0.1. The change in the Gibbs energy of the reaction in Eqs. (1) and (2) suggests that most likely, SiO gas is generated through a solid-solid reaction in the presence of direct contact between silica and carbon and between silica and silicon carbide[22]. While silicon is produced via solid-gas reaction in the contact between SiO and SiC. The optimum reduction temperature for silicon production is in a range from 1500℃ (1773K) to 1800℃ (2073K).

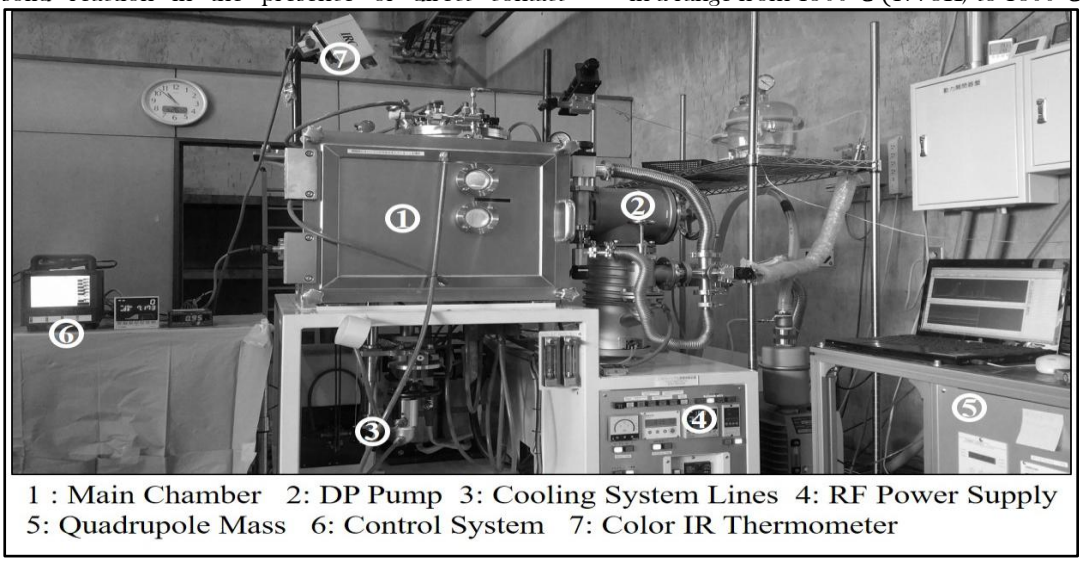

Fig. 3 Image of the induction heating furnace for the reduction process in this study.

2.2. Experimental Setup

Figure 3 shows the induction heating furnace of 30 kW power (Toei Scientific Industrial CO,. Ltd) used for carbothemal processioning. In the carbothermal reduction experiment, the gas species generating during the measurment were also investigated using quadrupole mass spectrometry (Q-mass) with direct connection to the induction furnace. Figure 4 shows a schematic illustration of the crucible setup in the present reseach. A high-purity graphite crucible with inner diameter of 40 mm and height of 70 mm was used for this study. Four mixture of silica (diameter 20~100um, Taiheiyo Cement Corporation Japan) and glassy carbon (diameter 20 um, Tokai Carbon, Ltd), were installed to the crucible with changing the molar ratio of siluca, graphite and silicon carbide as listed in table 1. The sample in the crucible was placed a the center of the induction furnance [16].

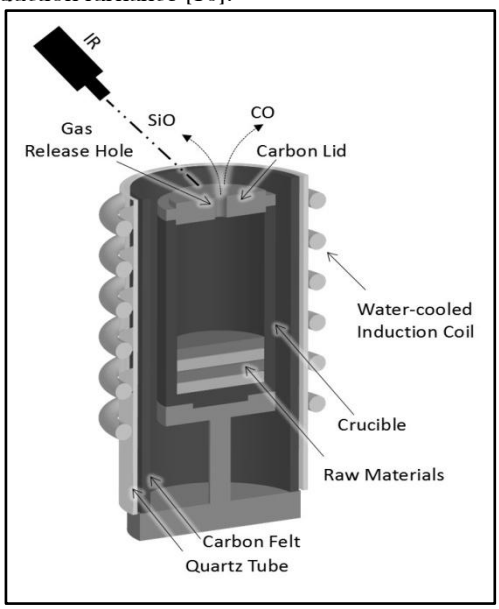

Fig. 4 Schematic figure of the crucible configuration.

The crucible was covered with carbon felt and surrounded by a quartz tube as insulation. The crucible temperature measured from the crucible top via infrared thermometer. The evacuation system of this appartus is composed of a rotary and diffusion pumps, which can reach to 10^{-3} Pa in a vacuum. During the heating experiment, the top temperature of the crucible was monitored by a high sensitive single color type infrared thermometer with a temperature range from 650℃ (923K) to 3500℃ (3773K) through the top glass window of the chamber. The induction coil heated the crucible with a frquency of 30 kHz under an open-loop control, and a quartz tube was placed in between the crucble and the coil for the protection of the crucible. The atmosphere during the heating process was pure argon gas (99.999%) with a pressure of 0.07 MPa to avoid the leak of the lethal carbon monoxide gas. The evacuation of the chamber to a higher vacuum order is required before the filing of the argon gas because the mass peaks between nitrogen and carbon monoxide are overlapped completely. The total pressure inside the chamber was recorded manually from the Bourdon gauge connected to the chamber.

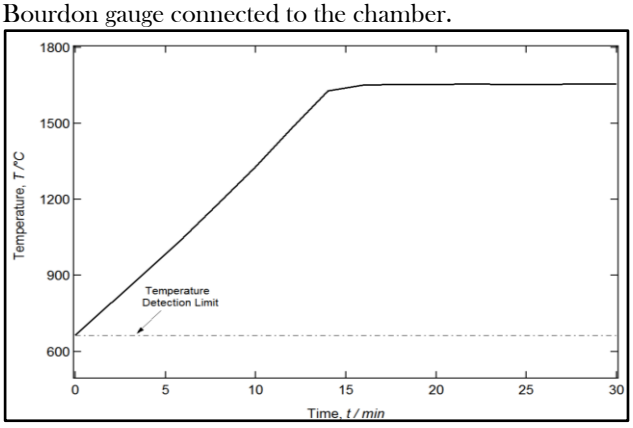

Fig. 5. The optimum used temperature was around 1650°C (1923K) recorded by the infrared thermometer during the reduction process. The detection range of the infrared thermometer is from 650°C to 3500°C.

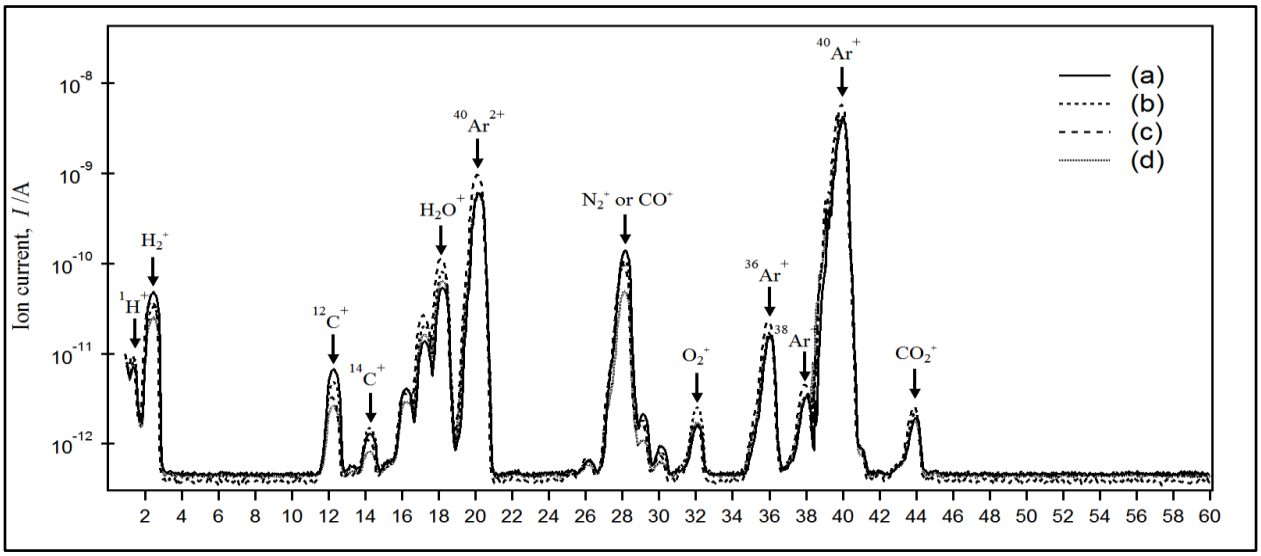

Fig. 6. Mass spectra of the chamber gases during the heating in case of four different silica to carbon ratios. A higher amounts of H_2O and O_2 were released when increasing the ratio of silica due to the presence of oxygen.

2.3. Method of Analysis

The analysis of x-ray diffraction (XRD) with a Cu-$K\alpha$ (λ = 1.5405 Å) radiation source over the angular range of $20° \leq 2\theta \leq 80°$ and a scan rate of 10°/min was employed by an x-ray diffractometer (SmartLab, Rigaku Corporation) to examine the phase composition. The system is equipated with a quadrupole mass spectrimeter (Q-mass) to analyze the chamber gas spectrometer and it can detect only CO gas because of the analysis in this study were performed at room temperature which is an impossible condition to detect SiO gas phase due to its low stability below 1300℃(1573K). The gas phase of SiO cannot reach the Q-mass analyzer because the Q-mass analyzer and the chamber are connected through a long metallic tube (inner diameter 0.711 mm) with an orifice. Therefore, the ratio of SiO gas to CO was calculated using the following equations:

$$M(\mathrm{CO})_{\mathrm{mol}} = P_{\mathrm{chamber}} * k * V_{\mathrm{chamber}} / R * T \quad \text{.....(6)}$$

where k is the maximum quadrupole intensity ratio between CO and Ar and it is plotted in Figure 7.

$$M(\mathrm{SiO})_{\mathrm{mol}} = (W_{\mathrm{Loss}} - M(\mathrm{CO})_{\mathrm{mol}} * 28)/44 \quad \text{.....(7)}$$

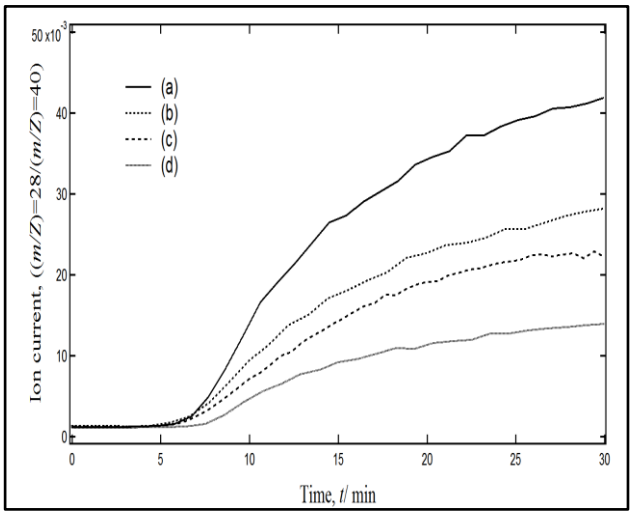

Fig. 7 (a, b, c and d) graphs representing the variation of released CO gas during the reduction process analyzed by quadrupole mass spectrometry, the highest released amount occurs in the case of (1.5, 1) ratio of silica to carbon as shown in (a).

3. Results and Discussion

3.1. Chamber Gas analysis

Figure 5 shows the temperature profile curves of the blank test as a typical temperatuere profile chosen and measured by the infrared thermometer in the pressent research work. For all the heating experiments the heating time was 30 minutes and the maxium temperature of the crucible was around 1650°C(1923K). The voltage and current of the induction coil, the temperature of the crucible were recorded by a data loger.

		a		b		c		d	
		(g)	(Si mol)	(g)	(Si mol)	(g)	(Si mol)	(g)	(Si mol)
SiO_2		6.160	0.103	6.360	0.106	6.560	0.109	6.660	0.111
C		0.840		0.640		0.440		0.340	
Total Mixture		7.000	0.103	7.000	0.106	7.000	0.109	7.000	0.111
SiC		1.300	0.033	1.300	0.033	1.300	0.033	1.300	0.033
Total Input		8.300	0.135	8.300	0.139	8.300	0.142	8.300	0.144
Total Product		2.729		1.918		1.590		1.205	
	Si	0.783	0.028	0.400	0.014	0.257	0.009	0.100	0.004
	SiC	1.940	0.049	1.500	0.038	1.330	0.033	1.100	0.028
Lost Gas		5.571		6.382		6.710		7.095	
	SiO	2.576	0.059	3.791	0.086	4.370	0.099	4.939	0.112
	CO	2.995		2.591		2.340		2.156	
Total Output		8.300	0.135	8.300	0.139	8.300	0.142	8.300	0.144
Si Yield (%)			20.7		10.3		6.5		2.8
SiC Yield (%)			35.9		27.0		23.5		19.1

Table 1 The mass balance of comparison between different ratios of SiO_2 to Carbon shows that the lower SiO gas loss, the more will be the amount of Si produced. The highest Silicon yield was achieved using the ratio of SiO_2 to carbon of (1.5, 1) as shown in the mass balance (a).

Figure 6 shows a compariosn of the quadrupole mass spectra between different molar ratios of silica to carbon. These results show that increasing the molar ratio of silica to carbon from 1.5 to 4 leaded to a release of a sginficant amount of H_2O and O_2 which is due to the additional O_2 gas contained on the solid form of SiO_2. While Figure 7 illustrates the temporal change of the relative mass peaks (m/Z = 28) which represents N_2/CO gasses and occurs mainly by the carbothermic reduction of silica. The intensity between the different molar ratio of silcia to carbon has a siginificant difference due to highe reactivity between silica and carbon in case of lower molar ratio (a), while in higher molar ratios (d) lack of carbon quantity leaded to less CO emission.

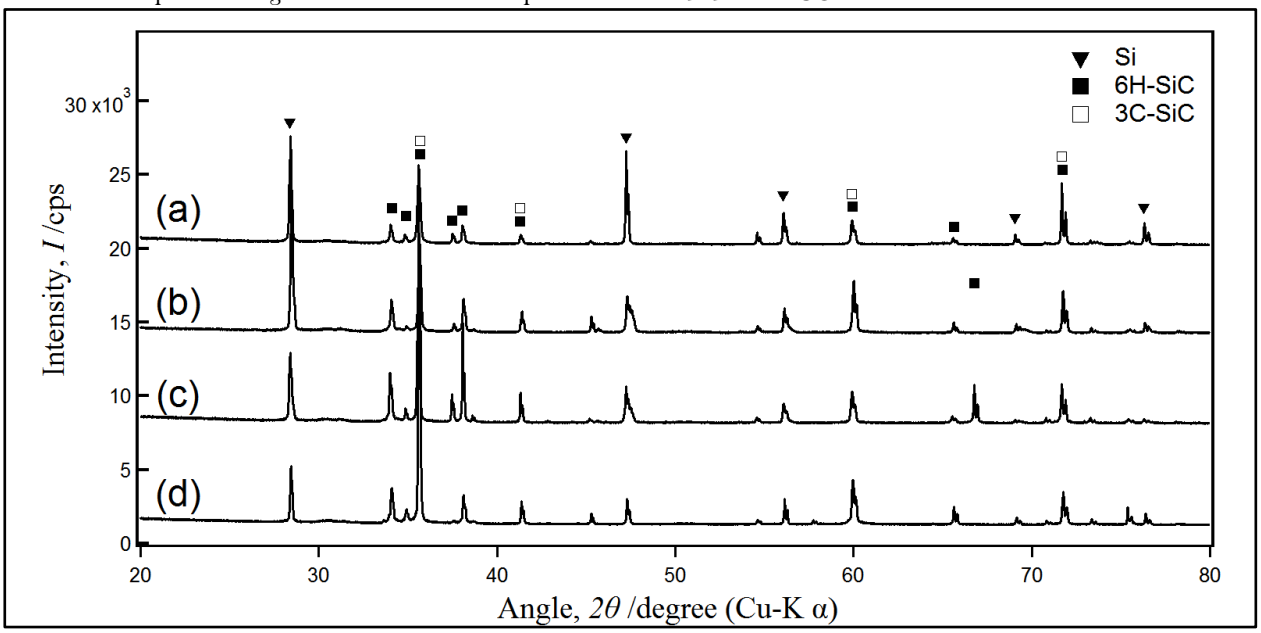

Fig. 8 X-ray diffraction patterns of obtained products for different raw material ratios.

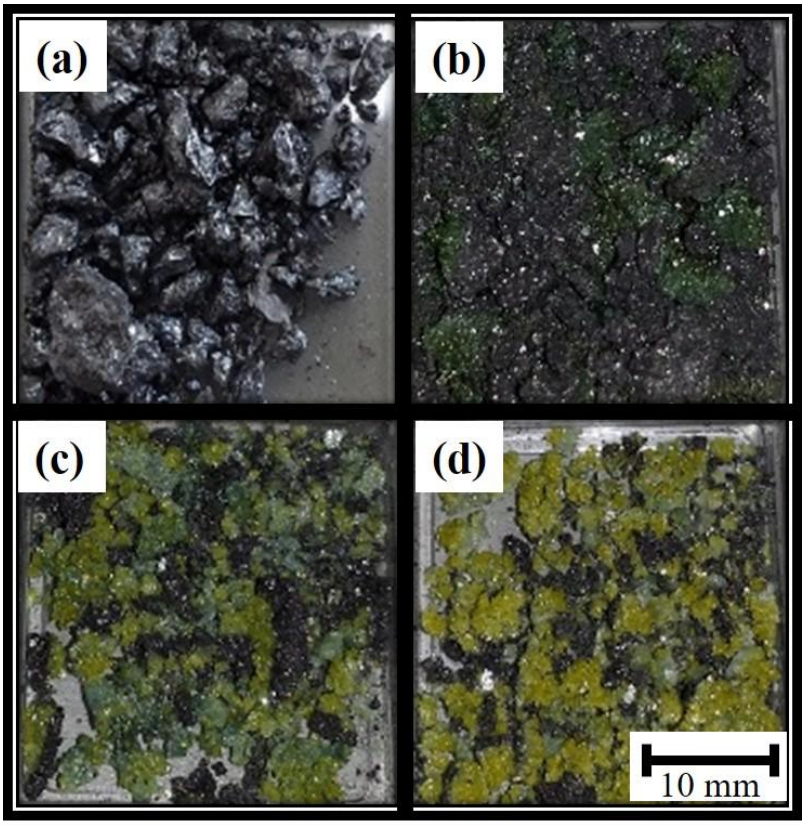

Fig. 9 Photos of the reduction product with four (SiO_2 : C) mixture ratios: (a) with (1.5, 1) showing solidified grey rocks of silicon mixed with silicon carbide, (b) with (2, 1) showing less solid form with obvious dark green colored material from silicon carbide, (c) with (3, 1) showing yellowish green product mixed with grey as proof of less amount of silicon, and (d) with (4, 1) showing mostly yellow colored product with almost no silicon

3.2. Product Analysis

Table 1 represents the mass balance, including the amount of input raw material, the product output and the weight loss as a gas phase in the case of each molar ratios. The Si product yield is defined as molar ratio of Si element in the product by the molar ratio of Si element in the input. The molar ratio 1.5 (a) between silica and carbon shows the highest Si yield of 20.7% compared to molar ratios (b), (c) of 10.3% and 6.5% while the lowest yield was observed when using the moalr ratio 4 represented by (d) and estimated by the powder diffraction patterns by the x-ray mille product as shown in Figure 8 which shown that the product included two phases of silicon carbide which are 6H-SiC and 3C-SiC with no peak mapped to silica or carbon in all XRD patterns which is consistent with the Si-C-O phase diagram discussed previously that the total consumption of silica and carbon was achieved in a temperature range from 1300K to 1900K. and proved by the different product obtained as illsutrated in Figure 9 which shows an image of the products in the case of the four different molar ratios, respectively. A grey solid rock image in case of (a) which represents the molar ratio of 1.5 can be explain by total reaction between silica and carbon raw material showing a higher yield of silicon (20.7%) and pure phase of silicon carbide (35.9%). In the case of (b), (c) and (d) molar ratio of 2, 3 and 4, respectively, the insuffisane of carbon was obvious leading to uncomplished reaction and illustrated by green and yellow colored material in the product which is different phase of silicon carbide, with less presence of silicon which agree with XRD results.

The decrease of Si yield in case of higher molar ratio between silica and carbon seems to be related to insufisance of carbon due to its exhaustion in the different redcution reactions as show in the phase diagram stability.

4. Conclusion

The phase stability diagram simulation of different reactions in the carbothermal reduction showed to be a powerful method for the estimation of the optimized reaction conditions such as temperature and partial pressure of the by-product gasses SiO and CO. Silicon was successfully obtained in a small-scale carbon crucible using an induction heating furnace with raw material powder form. Silicon production yield was improved by ten times via the optimization of the raw material input molar ratio between silica and carbon.

References

[1] H. C. Lee, S. Dhage, M. S. Akhtar, D. H. Kwak, W. J. Lee, C. Y. Kim and O. B. Yang: Curr. Appl. Phys. **10** (2010) S218–S221.

[2] E. Myrhaug and H. Tveit: El. Furnace Conf. **58** (2000).

[3] M. Stephen: PCT International Patent (1996) WO1996/041036.

[4] S. K. Iya, R. N. Flagella and F. S. Dipaolo: J. Electrochem. Soc. **129** (1982) 1531–1535.

[5] S. Wakamatsu and H. Oda: PCT International Patent (2001) WO2001/085613.

[6] H. S. N. Setty, C. L. Yaws, B. R. Martin and D. J. Wangler: U.S. Patent (1976) US 3,963,838.

[7] T. Homma, N. Matsuo, X. Yang, K. Yasuda, Y. Fukunaka and T. Nohira: Electrochim. Acta **179** (2015) 512–518.

[8] R. N. Andrews and S. J. Clarson: Silicon **7** (2015) 303–305.

[9] Y. Sakaguchi, M. Ishizaki, T. Kawahara,M. Fukai,M. Yoshiyagawa andF. Aratani: ISIJ Int. **32** (1992) 643–649.

[10] K. Itaka,T. Ogasawara,A. Boucetta,R. Benioub,M. Sumiya, T. Hashimoto,H. KoinumaandY. Furuya: J. Phys.: Conf. Ser. **596** (2015) 012015.

[11] R. K. Eckhoff: J. Loss Prev. Process Ind. **25** (2012) 448–459.

[12] R. K. Eckhoff: J. Loss Prev. Process Ind. **22** (2009) 105–116.

[13] S. V. Komarov, D. V. Kuznetsov, V. V. Levina and M. Hirasawa: Mater. Trans. **46** (2005) 827–834.

[14] E. Dal martello, G. Tranell, S. Gaal, O. S. Raaness, K. Tang, and I. Arnberg: Metall. Mater. Trans. **B42B** (2011) 939–950.

[15] L. P. Hunt, J. P. Dismukes and J. A. Amick: J. Electrochem. Soc. **131** (1982) 5–8.

[16] R. Benioub, A. Boucetta, A. Chahtou, S. M. Heddadj, M. Adnane, Y. Furuya and K. Itaka: Mater. Tran, JIM. 57 (2016) 1930-1935.

[17] H. Yokokawa, S. Yamauchi S and T. Matsumoto: Acta. Thermo.**245** (1994)45-55.

[18] S. V. Komarov, D. V. Kuznetsov, V. V. Levina and M. Hirasawa: Mater. Tran, JIM. **46** (2005) 827-834.

[19] M. Tada and M. Hirasawa: High Temp. Mater. Proc. **19** (2000) 281-297.

[20] A. W. Weimer, K. J. Nilson, G. A. Cochran and R. P. Roach: J. AIChE. **39** (1993) 493-503.

[21] T. Kikuchi, T. Kurosawa and T. Yagihashi: Mater. Tran, JIM. **32** (1968) 866-872.

[22] D. H. Filsinger and D. B. Bourrie: J. Am. Ceram. Soc. **73** (1990) 1726–1732.